

Domains and domain walls in graphite intercalation compounds

Hyangsuk Seong and Surajit Sen

Department of Physics and Astronomy, Michigan State University, East Lansing, Michigan 48824

Tahir Çağın

*Molecular Simulations Incorporated, 199 S. Robles Avenue, Pasadena, California 91101
and Beckman Institute, California Institute of Technology, Pasadena, California 91125*

S. D. Mahanti

Department of Physics and Astronomy, Michigan State University, East Lansing, Michigan 48824

(Received 23 September 1991)

The structure of domains and domain walls in the low-temperature solid phase of stage-2 alkali-metal graphite intercalation compounds is studied using molecular dynamics (MD) simulation and a model potential obtained from fitting to the liquid structure data. For RbC_{24} , we find small domains of $(\sqrt{7} \times \sqrt{7})$ structure containing mostly seven Rb atoms and with domain walls consisting of (2×2) and (2×3) elemental placquettes. These nanostructures provide a clear picture of the discommensurations and a consistent understanding of the x-ray-diffraction measurements. Based on the simulation results we propose a periodic domain-wall model that explains very well the dominant features of the x-ray structure factor for both RbC_{24} and CsC_{24} when we allow for small changes in the planar density.

Structural and dynamic properties of systems with competing interactions continue to be one of the most interesting areas of condensed-matter physics.¹ Of particular interest over the past decade has been the study of structural properties of binary and ternary graphite intercalation compounds (GIC's).^{2,3} Considerable amount of experimental^{2,3} and theoretical⁴ work has helped in elucidating many of the interesting physical properties of these systems. One area where a detailed microscopic understanding is still lacking is the incommensurability of stage- n ($n \geq 2$) GIC's containing Cs, Rb, and K ions as intercalants. In this paper we address this issue by probing the structure of domains and domain walls using molecular dynamics (MD) simulations and then propose a simple model for the low-temperature structure of the alkali-metal GIC's.

Stage- n GIC's are characterized by a stacking sequence of graphitic and intercalant layers in which the neighboring intercalant layers are separated by n graphitic layers. The intercalant ions interact predominantly via screened Coulomb repulsion and are affected by an effective one-particle corrugation potential produced by the graphite layers. Thus, these systems exhibit a competition between two length scales, periodicity of the substrate corrugation potential and the average separation between the intercalant ions controlled by their layer density (ρ). In addition, there is also a competition between two energy scales, the depth of the corrugation potential and the interaction energy/particle which is determined by ρ and the strength of the interparticle interaction.

In the stage-1 GIC's of K, Rb, and Cs, the intercalants form a commensurate triangular $(2 \times 2)R0^\circ$ structure where $R0^\circ$ and (2×2) imply that the unit-cell vectors of the intercalant superlattice are parallel to the graphite unit cell (**a**,**b**) and are twice as large. The layer stoichiometry is MC_8 , where M stands for the intercalant and C for the carbon (note there are two carbon atoms per graphite unit cell). This gives $\rho = \frac{1}{4}$ [in units of $1/(\text{area of the graphite unit cell})$]. In contrast, structures of stage- n ($n \geq 2$) systems are more intriguing. Chemical stoichiometry of these compounds is in general MC_{12n} and the layer stoichiometry is MC_{12} , giving $\rho = \frac{1}{6}$. In the absence of the corrugation potential, the ground state is a triangular lattice with arbitrary orientational epitaxy angle ϕ (measured with respect to graphite a^* axis, also known as Novaco-McTague angle⁵). A question of fundamental interest is the effect of corrugation both on the intercalant structure and the intercalant dynamics.

The liquid state structure in stage-2 compounds is well understood through the careful MD work of Moss and co-workers⁶⁻⁸ and Chen, Karim, and Pettitt⁹ in terms of a highly structured liquid close to the liquid-solid phase transition. The nature of the solid structure, however, is not as well understood although qualitative models have been proposed by Clarke and co-workers^{10,11} for MC_{24} ($M = \text{Cs, Rb, and K}$) in terms of different types of commensurate domains separated by discommensurations (domain walls). Also Ginzburg-Landau models have been proposed to understand the domain structure.¹²⁻¹⁴ From x-ray-diffraction measurements in CsC_{24} and RbC_{24} , Clarke and co-workers^{10,11} suggested the coexistence of commensurate $(\sqrt{7} \times \sqrt{7})$ and (2×2) regions. They explained their diffraction results for Cs by postulating the coexistence of $(\sqrt{7} \times \sqrt{7}) R\phi$ domains with $\phi = \pm 19.11^\circ$. The commensurate domains were $\sim 40 \text{ \AA}$ in size containing about 30 Cs atoms along with narrow domain walls oriented parallel to the graphite (110) directions (see Fig. 3 in Ref. 10). However, they neither discussed the precise nature of the domain walls nor analyzed the spatial distributions of $(\sqrt{7} \times \sqrt{7})$ and 2×2 domains which is necessary

to satisfy the density constraint for their postulate. In the case of RbC_{24} , it was not quite clear whether (2×2) domains were present or not.

Following the suggestions of Clarke *et al.*,¹⁰ several theoretical studies based on Ginzburg-Landau theory of incommensuration in the incommensurate phase were carried out pointing out the importance of third-order terms in stabilizing the $(\sqrt{7} \times \sqrt{7})$ domains.¹²⁻¹⁴ These theories were able to explain the observed Novaco-McTague angle ϕ and intensities of the higher-order superlattice reflections semiquantatively, although they did not address the structure of the domain walls in detail. As we will show later, *domain and domain-wall sizes in these systems are comparable* and one should therefore also know the microscopic structure of the walls.

MD calculations were carried out for RbC_{24} using the potential model of Ref. 9. The one-particle corrugation potential in this model was obtained by Moss *et al.*⁶ by fitting to the liquid structure factor $S(\mathbf{k})$ and is given by

$$V_1(r) = 2K[2 \cos(2\pi x/a) \cos(2\pi y/\sqrt{3}a) + \cos(4\pi y/\sqrt{3}a)]. \quad (1)$$

In Eq. (1), $2K/k_B = -270$ K and a ($a = 2.46$ Å) is the graphite unit-cell constant. The two-body potential is given by

$$V_2 = q^2 \sum_{i,j} \exp(-\Gamma r_{ij})/r_{ij}, \quad (2)$$

with $q = 4.8028 \times 10^{-10}$ esu and $\Gamma = 0.49$ Å⁻¹.

The above potential has successfully reproduced the liquid structure data at 250 K. We have repeated the MD simulations at this temperature using both constant energy and constant temperature algorithms and our results agree with the earlier results of Chen, Karim, and Pettitt.⁹ Before discussing the solid structure results, let us discuss some energetics. The strength of the corrugation potential as measured by $V_1^{\text{saddle}} - V_1^{\text{min}} = 1080$ K, i.e., we are in the strong to intermediate corrugation limit for $T < 300$ K. The energy/particle for different commensurate structures are 17742 K ($\sqrt{3} \times \sqrt{3}$); 9825 K (2×2); 4476 K (2×3); 3114 K ($\sqrt{7} \times \sqrt{7}$). Although the (2×3) structure has the correct layer density, the lower energy of the $(\sqrt{7} \times \sqrt{7})$ structure favors the latter.

MD simulations were performed with 216 and with 864 Rb ions distributed to insure a planar density of $\rho = \frac{1}{6}$ and with 301 Rb ions for a slightly different density of $\rho = 1/6.15$. The MD cell edges were arranged to lie on the corrugation minima and periodic boundary conditions were imposed. MD equations were solved using sixth-order Gear predictor-corrector algorithm. The time step was taken to be 0.0028 ps and equilibration times of at least 170 ps and 1 ns were used for the 216- and 864-particle systems, respectively. In the case of constant energy simulations the energy/ion was noted to be conserved to 99.82% accuracy for the smaller system over the entire run periods. The solid state was reached via slow cooling in steps of 10 K from the liquid state. Here we report our results for two temperatures, 250 (liquid) and 3 K (solid). The details of the phase transition will be given in a more detailed publication.¹⁵

In Figs. 1(a) and 1(b) we give the spherically averaged

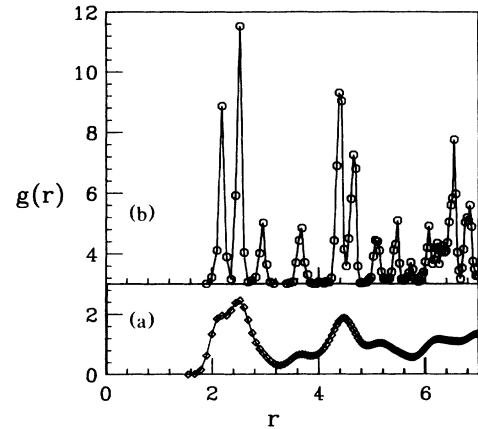


FIG. 1. Pair correlation function $g(r)$ for RbC_{24} as a function of r (in units of graphite lattice constant $a = 2.46$ Å) for (a) the liquid at 250 K and (b) the solid at 3 K for the 216-particle system. Note that the zero for the solid is 3.0.

real space pair distribution function $g(r)$ for the liquid and the solid. Clearly, the liquid is strongly perturbed by the substrate and is *structured*, as noted earlier by Fan *et al.*⁷ and Chen, Karim and Pettitt⁹ following the earlier suggestion by Parry¹⁶ for CsC_{24} . The solid phase $g(r)$ shows three distinct peaks at 2.19, 2.53, and 2.97 (in units of graphite unit-cell length a) and these can be related to distances of 2, $\sqrt{7}$, and 3, respectively.¹⁷ A similar three-peak structure was obtained from a Monte Carlo study of Plischke and Leckie.¹⁸ This three-peak structure suggests that the system may show coexisting domains of $(\sqrt{7} \times \sqrt{7})$ and (2×2) consistent with the picture proposed by Clarke *et al.*¹⁰ for CsC_{24} . The positions of the intercalant atoms joined by lines connecting nearest neighbors using Voronoi polyhedra constructions are shown in Figs. 2(a) and 2(b) corresponding to two different concentrations of Rb atoms (RbC_{24} and $\text{RbC}_{24.57}$). In contrast to the picture of Clarke *et al.* for CsC_{24} [presence of large domains of $(\sqrt{7} \times \sqrt{7})$ structure containing about 30 atoms oriented in different directions and separated by narrow domain walls of unknown atomic structure], we see placquettes of $(\sqrt{7} \times \sqrt{7})$ structure consisting mostly of 7 atoms (we will call these nanodomains)

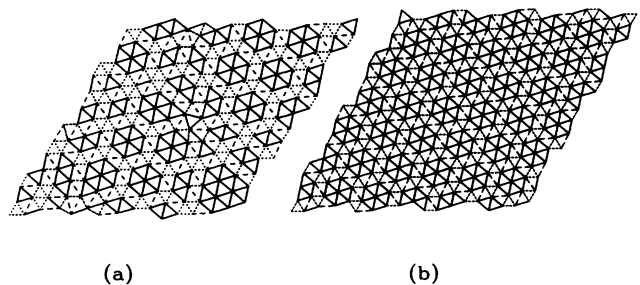


FIG. 2. Solid structure of (a) RbC_{24} and (b) $\text{RbC}_{24.57}$. The solid, dotted, and dashed lines correspond to the nearest-neighbor distances near $\sqrt{7}$, 2, and 3 (in units of graphite lattice constant), respectively.

for RbC_{24} [Fig. 2(a)]. The intersection of three such placquettes form a triangular placquette of (2×2) structure containing 3 atoms. The wall between two $(\sqrt{7} \times \sqrt{7})$ nanodomains consists of $(2 \times 3 \times \sqrt{7})$ triangular placquettes which give rise to the peak near 3 in $g(r)$. These domain walls should also give a peak corresponding to r near $\sqrt{13} = 3.6$ which we find [see Fig. 1(b)]. Our MD simulations give a picture rather similar to the one suggested by Zabel *et al.*¹⁹ for RbC_{24} (see their Fig. 1 and also see figures in Ref. 20). In fact, by choosing a slightly smaller density of Rb ions we see a perfectly ordered arrangement of $\sqrt{7} \times \sqrt{7}$ domains with (2×3) domain walls.

To compare the MD results with x-ray-diffraction measurements we calculate the structure factor $S(\mathbf{k})$ for the atomic positions given in Fig. 2(a). The structure factor for the solid phase (216-particle system) is given in Fig. 3. The liquid state $S(\mathbf{k})$ at 250 K (not given in the figure) shows clearly the effect of corrugation with peaks at \mathbf{k} corresponding to the reciprocal-lattice vectors of the graphite substrate and the dominant peak at $k = 1.2 \text{ \AA}^{-1}$ corresponding to an incommensurate liquid.²¹ The solid $S(\mathbf{k})$ shows three discernible peaks denoted by I_1 , I_2 , and I_3 . The k values and angles of the two stronger peaks measured from the graphite \mathbf{a}^* axis are given in Table I along with the available experimental values and predictions of the periodic domain-wall model to be described below.

Our MD simulation gives two prominent peaks (I_1 and I_2) which have the same $k = 1.21 \text{ \AA}^{-1}$ but different angles with respect to the graphite \mathbf{a}^* axis. The angle associated with the dominant peak I_1 , ϕ , is 10.2° whereas that associated with the weaker peak I_2 which we denote as ψ is 35.8° . The strengths of these two peaks are 0.52 and 0.052, respectively. There is a third peak I_3 ($k = 1.40 \text{ \AA}^{-1}$, the angle with the \mathbf{a}^* axis is 7.6°) which is weak (strength 0.015) and will not be discussed any further.

Clarke *et al.*¹⁰ saw two peaks similar to I_1 and I_2 in CsC_{24} (1 and 2 in their notation in Ref. 10). The corresponding k and angles ϕ and ψ are given in Table I. In addition, they also saw a peak as strong as I_1 ($1'$ in their notation) which originated from the rotational equivalent of I_1 corresponding to $-\phi$. The origin of the low intensity peak I_2 was ascribed to the interdomain scattering associated with the coexistence of two different orientations of $(\sqrt{7} \times \sqrt{7})$ commensurate domains. Our MD simulations show only one orientation of these domains (either 1 or $1'$) thus indicating that it is not necessary to invoke domains with different orientations to explain the origin of the I_2 peak. It is sufficient to have domain walls, in our case the

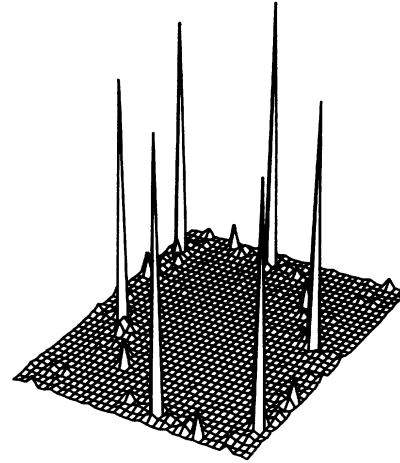


FIG. 3. X-ray structure factor $S(\mathbf{k})$ for RbC_{24} at 3 K obtained from MD simulations for the 216-particle system. Only the dominant peaks I_1 , I_2 (see text), and their sixfold symmetry counterparts are clearly visible.

two domains sandwiching a wall being simply shifted with respect to one another by a lattice vector of the underlying graphite lattice. For RbC_{24} the dominant peak I_1 ($k = 1.22 \text{ \AA}^{-1}$, $\phi = 10.1^\circ$) (Ref. 10) is in good agreement with our MD results. The lower intensity peak (I_2) for this system was not discussed in Ref. 11 but the corresponding angle ψ agrees very well with the diffraction results of Rousseaux *et al.*²²

To understand more about the physical origin of the two peaks discussed above, we propose a periodic domain wall (PDW) model which consists of periodic arrays of commensurate $(\sqrt{7} \times \sqrt{7})$ domains of total width $2L$ (all of same orientation) interspersed by domain walls of width M . The domain walls consist of (2×3) regions and the region where three domains meet consist of triangular arrays of (2×2) structure [see Fig. 2(b)]. In this model one goes from the commensurate $(\sqrt{7} \times \sqrt{7})$ structure ($M = 0$, arbitrary L) to the commensurate (2×2) structure (arbitrary M , $L = 0$). For arbitrary (L, M) the superlattice unit cell is obtained by joining the centers of the $(\sqrt{7} \times \sqrt{7})$ domains and the unit-cell vectors are given by $\mathbf{A} = 2(2L + M)\mathbf{a} + L\mathbf{b}$, and $\mathbf{B} = -L\mathbf{a} + (5L + 2M)\mathbf{b}$. The layer density is determined by (L, M) . Our MD simulations suggest that RbC_{24} can be described very well by the PDW model with $L = M = 1$ (this corresponds to the

TABLE I. Comparison of angles and peak positions of $S(\mathbf{k})$ between experiment (Expt.), molecular dynamics (MD), and periodic domain-wall model (PDW) (see text). ϕ is the Novaco-McTague angle; ψ is the angle of the peak produced by interdomain scattering (angle of I_2 in Ref. 11); $k_\phi = k_\psi = k_p$ is the magnitude of \mathbf{k} at angles ϕ and ψ .

	Expt.	ϕ (ψ) MD	PDW	Expt.	$k_\phi = k_\psi = k_p$ MD	PDW
RbC_{24}	10.1 (35.5)	10.2 (35.8)	11.5 (33.3) ^a	1.22	1.21	1.19 ^a
CsC_{24}	14.5 (28)	· · · (· · ·)	14.5 (27.6) ^b	1.16	· · ·	1.15 ^b

^aFor $L = M = 1$ ($\text{RbC}_{24,57}$).

^bFor $L = 2$, $M = 1$ ($\text{CsC}_{26,1}$).

stoichiometry $\text{RbC}_{24.57}$), with a small number of defects. To study this, we studied a 301-particle system with smaller density of Rb's corresponding to $\text{RbC}_{24.57}$ and its low-temperature structure is given in Fig. 2(b). The structure factor for the defect-free case has been calculated exactly and the corresponding values of k , angles, and the strengths of the two peaks (I_1, I_2) are (1.19, 1.19) \AA^{-1} , ($11.5^\circ, 33.3^\circ$), and (0.573, 0.137), respectively. The larger value of the intensity of the I_2 peak in the PDW model (0.137) for $\text{RbC}_{24.57}$ compared to the MD results (0.052) for RbC_{24} is due to the perfect ordering of the Rb ions in the PDW model.

We find by actual calculation that the epitaxy angles ϕ and ψ satisfy the relation $\sin\psi = \sqrt{3}\sin(30 - \phi)$ for the PDW model with $M=1$ and arbitrary L . In the limit $L \rightarrow \infty$, this relation gives $\phi = \psi = 19.1^\circ$, i.e., the two peaks merge with each other for the commensurate ($\sqrt{7} \times \sqrt{7}$) case. Furthermore, the CsC_{24} results of Clarke *et al.*¹⁰ can be approximated by the $L=2, M=1$ PDW model which corresponds to a stoichiometry $\text{CsC}_{26.1}$, and gives $k=1.15 \text{ \AA}^{-1}$, $\phi=14.5^\circ$, $\psi=27.6^\circ$ in excellent agreement with the experimental values 1.16 \AA^{-1} , 14.5° , and 28° , respectively. The corresponding intensities in the PDW model are respectively 0.568 and 0.144 and the number of Cs atoms in a domain is 19.

In summary, the potential obtained by fitting the struc-

ture factor in the liquid state can be successfully applied to the study of the low-temperature microstructure in alkali-metal GIC's. The success of the chosen potential is confirmed by the agreement between the experimental $S(\mathbf{k})$ and that obtained from our simulations for RbC_{24} . We also find that the simulated $S(\mathbf{k})$ for the stage-2 GIC closely agrees with the experimental $S(\mathbf{k})$ for stage-3 systems.¹¹ This observation confirms our original assumption concerning weak interlayer coupling and effective two dimensionality of these alkali-metal GIC's. Simulations suggest that the real space structure of the Rb lattice consists of thick domain walls lining the domains with length scales comparable to the domain walls. Finally, our $S(\mathbf{k})$ calculations for the $L=2, M=1$ PDW model which recognizes the importance of the domain walls shows remarkable agreement with experimental $S(\mathbf{k})$ for the stage-2 Cs GIC. This last success indicates that the PDW model describes very well the main features of the low-temperature structure of the stage-2 and higher-stage GIC's of RB and Cs.

We thank Professor M. F. Thorpe for useful discussions. This work was partially supported by NSF Grants No. DMR-MRG 89-035799 and No. DMR 90-24955, and the Center for Fundamental Materials Research.

¹Competing Interactions and Microstructures: Statics and Dynamics, edited by R. LeSar, A. Bishop, and R. Hefner (Springer, Berlin, 1988).

²Graphite Intercalation Compounds, Vol 1: Structure and Dynamics, edited by H. Zabel and S. A. Solin, Springer Series on Topics in Current Physics (Springer, Berlin, 1990).

³S. A. Solin and H. Zabel, Adv. Phys. **37**, 87 (1988).

⁴S. A. Safran, in Solid State Physics, edited by H. Ehrenreich and D. Turnbull (Academic, New York, 1987), Vol. 40.

⁵A. D. Novaco and J. P. McTague, Phys. Rev. Lett. **38**, 1286 (1977).

⁶S. C. Moss *et al.*, Phys. Rev. Lett. **57**, 3191 (1986).

⁷J. D. Fan, Omar A. Karim, G. Reiter, and S. C. Moss, Phys. Rev. B **39**, 6111 (1989).

⁸J. D. Fan, George Reiter, and S. C. Moss, Phys. Rev. Lett. **64**, 188 (1990).

⁹Zhuo-Min Chen, Omar A. Karim, and B. Montgomery Pettitt, J. Chem. Phys. **89**, 1042 (1988).

¹⁰R. Clarke, J. N. Gray, H. Homma, and M. J. Winokur, Phys. Rev. Lett. **47**, 1407 (1981).

¹¹M. J. Winokur and R. Clarke, Phys. Rev. Lett. **54**, 811 (1985).

¹²Y. Yamada and I. Naiki, J. Phys. Soc. Jpn. **51**, 2174 (1982).

¹³M. Suzuki and H. Suematsu, J. Phys. Soc. Jpn. **52**, 2761 (1983).

¹⁴M. Suzuki, Phys. Rev. B **33**, 1386 (1986).

¹⁵Hyangsuk Seong, S. D. Mahanti, Surajit Sen, and Tahir Çağın (unpublished).

¹⁶G. Parry, Mater. Sci. Eng. **31**, 99 (1977).

¹⁷Surajit Sen, Tahir Çağın, Hyangsuk Seong, and S. D. Mahanti, in Recent Developments in Computer Simulation Studies in Condensed Matter Physics IV, edited by D. P. Landau *et al.* (Springer, Berlin, 1991).

¹⁸M. Plischke and W. D. Leckie, Can. J. Phys. **60**, 1139 (1982).

¹⁹H. Zabel *et al.*, Phys. Rev. Lett. **57**, 2041 (1986).

²⁰S. C. Moss, and R. Moret, in Graphite Intercalation Compounds, Vol. 1: Structure and Dynamics (Ref. 2), p. 58.

²¹H. Zabel, A. Magerl, J. J. Rush, and M. E. Misenheimer, Phys. Rev. B **40**, 7616 (1989).